

## Structure and electronic properties of FeSi<sub>2</sub>

S. J. Clark, H. M. Al-Allak, S. Brand, and R. A. Abram

*Department of Physics, University of Durham, Science Laboratories, South Road, Durham DH1 3LE, United Kingdom*

(Received 13 May 1998)

The nature of the band gap in the semiconducting material  $\beta$ -FeSi<sub>2</sub> is still under some dispute. Although most experimental results indicate the band gap to be direct, *ab initio* work generally reports the material to be an indirect semiconductor with the direct transition a few tens of millielectron volts higher than the indirect gap. However,  $\beta$ -FeSi<sub>2</sub> is commonly grown epitaxially on a diamond-structure Si substrate, and as a consequence, the  $\beta$ -FeSi<sub>2</sub> unit cell is strained. Here we report the results of *ab initio* density-functional calculations, which we have performed on  $\beta$ -FeSi<sub>2</sub> where its lattice parameters are constrained according to the heteroepitaxial system  $\beta$ -FeSi<sub>2</sub>(100)/Si(001). This forms two types of lattice matching: (A)  $\beta$ -FeSi<sub>2</sub>[010]||Si<110> and (B)  $\beta$ -FeSi<sub>2</sub>[010]||Si<001>. We find that the  $\beta$ -FeSi<sub>2</sub> band gap is highly sensitive to its lattice parameters and therefore to the orientation at which the material is grown on silicon. We find that type A favors a more direct band gap, while type B has an indirect gap. [S0163-1829(98)05039-5]

### I. INTRODUCTION

$\beta$ -FeSi<sub>2</sub> is a semiconductor with a band gap of  $\sim 0.83$ – $0.87$  eV at room temperature<sup>1,2</sup> (corresponding to the minimum-absorption window of silica-based fibers) making it a potential candidate for the use in near infrared detectors and light emitters. The crystal structure of  $\beta$ -FeSi<sub>2</sub> (Ref. 3) is base-centered orthorhombic (space group *Cmca*) having 48 atoms per unit cell and lattice parameters  $a = 9.863$  Å,  $b = 7.884$  Å, and  $c = 7.791$  Å. The unit cell has two inequivalent Fe sites, each occupied by 8 atoms as well as two inequivalent Si sites with 16 atoms in each. Even though there is no simple lattice parameter match, epitaxial layers of  $\beta$ -FeSi<sub>2</sub> can be grown easily on Si(001) and Si(111) substrates using a variety of techniques such as, molecular beam epitaxy,<sup>4</sup> chemical vapor deposition,<sup>5</sup> electron beam deposition,<sup>6</sup> and metal-organic vapor phase epitaxy.<sup>7</sup> Buried epilayer of the material have also been successfully realized by ion beam synthesis.<sup>8</sup> The possible compatibility of  $\beta$ -FeSi<sub>2</sub> with standard silicon processing technology and its potential optoelectronic capabilities, has recently generated considerable interest in the properties of this material.

However, despite the large amount of work reported in the literature, the nature of the band gap of  $\beta$ -FeSi<sub>2</sub> is still controversial. *Ab initio* calculations performed by a number of workers, suggested that there exists an indirect band gap a few millielectron volts less than the direct one at the *Y* point in the Brillouin zone. Augmented spherical wave calculations performed by Eppenga<sup>9</sup> gave a direct band gap of 0.46 eV and an indirect gap of 0.44 eV. The oscillator strengths for optical transitions across the gap at  $\Gamma$  were found to be small but become significant for photon energies around 0.77 eV, which is close to the experimental band gap. From linear muffin-tin orbital (LMTO) calculations, Christensen<sup>10</sup> obtained a direct band gap of 0.8 eV and an indirect gap of  $\sim 0.77$  eV (as deduced from his band diagram). The work also demonstrated the sensitivity of the states at the band edge to the atomic positions, as minor displacement of the Fe atoms in the unit cell was found to lead to significant changes in the calculated band gap. Full-potential linear aug-

mented plane wave calculations carried out by Eisebitt *et al.*,<sup>11</sup> revealed a direct gap of 0.78 eV at a point of low symmetry (along the  $Z\Gamma$  line) and a slightly larger direct gap of 0.82 eV at the *Y* point. The work of Filonov *et al.*<sup>12</sup> using the LMTO method with different atomic sphere radii on different sites, showed a direct band gap of 0.74 eV. However, their experimental measurements of the absorption coefficients of  $\beta$ -FeSi<sub>2</sub> revealed the presence of both direct and indirect gaps and concluded that the material is a quasidirect semiconductor, where the direct gap does not occur at a point of high symmetry. Electronic structure calculations performed by van Ek, Turchi, and Sterne<sup>13</sup> with the LMTO method in the atomic-sphere approximation resulted in an indirect gap of 0.44 eV and a direct gap of 0.51 eV. A recent<sup>14</sup> LMTO calculation using the atomic-sphere approximation again resulted in an indirect band gap of 0.44 eV followed by a slightly larger direct gap of 0.52 eV. On the other hand, their reflectivity measurements revealed the onset of absorption only at 0.8 eV. This was attributed to a low oscillator strength due to the *d*-like nature of the states in the region of the direct gap.

Only few experimental results<sup>15,16</sup> seem to indicate the existence of an indirect transition. Photoluminescence emission, which indicates a direct gap transition, has been reported by a number of workers for  $\beta$ -FeSi<sub>2</sub> layers grown by a variety of techniques.<sup>2-5,17</sup> More recently Leong *et al.*<sup>18</sup> have successfully fabricated a light emitting device operating at a wavelength of 1.5  $\mu$ m that incorporates  $\beta$ -FeSi<sub>2</sub> into a conventional silicon bipolar junction, by growing a buried  $\beta$ -FeSi<sub>2</sub> epilayer on a Si(001) substrate. One possible explanation why the experimental results generally indicate the existence of a direct band gap may be related to the fact that the material investigated is usually in the form of a thin film grown on a silicon substrate. In this case the degree of strain in the film will also play an important role in the apparently direct nature of the optical transitions.

In this paper we have calculated the electronic structures of bulk and strained  $\beta$ -FeSi<sub>2</sub> epilayers grown on Si(001) surfaces, using a plane-wave density-functional method. The use of a Si(001) substrate was found to result<sup>19</sup> in the het-

eroepitaxial relationship  $\beta$ -FeSi<sub>2</sub>(100)/Si(001) with two types of lattice matching: (A)  $\beta$ -FeSi<sub>2</sub>[010]||Si<110> and (B)  $\beta$ -FeSi<sub>2</sub>[010]||Si<001>. Consequently, two strained unit cells corresponding to type A and type B matching were considered. As a result of this work, we show that the type-A orientation favors a more direct band gap.

## II. DETAILS OF THE CALCULATIONS

For each structure of  $\beta$ -FeSi<sub>2</sub> considered here we have performed *ab initio* density-functional calculations within the pseudopotential and generalized gradient approximations (GGA).<sup>23</sup> The GGA for the exchange and correlation potential is used here in preference to the more commonly used local-density approximation (LDA) (Ref. 24) since it does not underestimate band gaps to the same extent as the LDA. However, with both the LDA and the GGA, the trends in gap properties tend to be reliable.

We construct the primitive unit cell and expand the valence electronic wave functions in a plane-wave basis set up to an energy cutoff of 560 eV, which converges the total energy of the unit cell to better than 1 meV/atom. In the total-energy calculations, integrations over the Brillouin zone were performed by using a  $4 \times 4 \times 4$  Monkhorst-Pack<sup>20</sup> set, which gives 8 symmetrized  $k$  points, again converging total energies to better than 1 meV/atom. A preconditioned conjugate gradients routine<sup>25</sup> was used to minimize the energy of the electronic system. Electron-ion interactions are described by a  $Q_c$ -tuned pseudopotential<sup>22</sup> in the Kleinman-Bylander form.<sup>21</sup> The Hellmann-Feynman theorem was employed to calculate the forces on the atoms and we also used a conjugate gradients routine to relax the atomic positions. The lattice parameters of the structure were also optimized (under the given constraints for each calculation). When a plane-wave basis set is used to calculate the stresses on the cell, a Pulay correction is included in the stress and total energy, which compensates for the changing basis set as the unit cell changes shape.

Following the relaxation of the electronic and geometric structure, the band structures of the various  $\beta$ -FeSi<sub>2</sub> cells are calculated. For this we use the self-consistent charge density obtained from the relaxation calculations to construct the Hamiltonian of the system and diagonalize it at various points in the Brillouin zone to obtain the energy eigenvalues.

## III. STRUCTURE OF THE $\beta$ -FeSi<sub>2</sub>/Si INTERFACES

The  $\beta$ -FeSi<sub>2</sub>(100)/Si(001) interface exhibits two types of azimuthal orientations which we shall label as type A and type B. The lattice parameter of Si is  $a = 5.43$  Å, so we define a tetragonal unit cell of the diamond structure with crystal-translation vectors  $a'$ ,  $b'$ , and  $c'$  such that  $a' = (1, -1, 0)a$  (which is 7.6792 Å at 45° to the conventional cubic axes) and  $b' = (1, 1, 0)a$ . The perpendicular axis  $c' = (0, 0, 1)a$  is unchanged with respect to the original cell. It can be seen that the surface unit cell in the interfacial (001) plane of the new Si cell gives a good match to that of  $\beta$ -FeSi<sub>2</sub> in the [100] plane since, for  $\beta$ -FeSi<sub>2</sub>,  $b = 7.791$  Å and  $c = 7.833$  Å. This gives a maximum-lattice mismatch of 1.8% for the  $\beta$ -FeSi<sub>2</sub> [100] plane against the Si [001] plane in the <110> direction where the  $\beta$ -FeSi<sub>2</sub> is

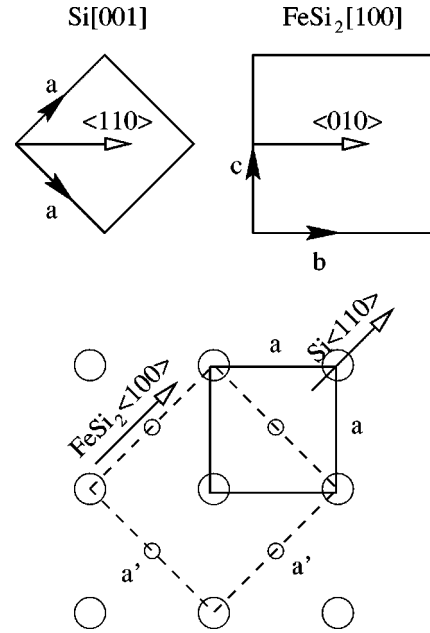


FIG. 1. The type-A ( $\beta$ -FeSi<sub>2</sub>[010]||Si<110>) heteroepitaxial relationship. The top diagram shows plan views of the conventional Bravais lattices of Si and  $\beta$ -FeSi<sub>2</sub>. In the bottom diagram the top layer of atoms in the Si cell are shown as open circles and a  $\beta$ -FeSi<sub>2</sub> cell (dashed lines) is chosen to coincide with the Si conventional cell, given a  $\pi/4$  rotation around the direction perpendicular to the substrate.

slightly compressed with respect to the bulk lattice. This is the type-A heteroepitaxial relationship and is illustrated in Fig. 1 where schematics of the  $\beta$ -FeSi<sub>2</sub> and Si unit cells are shown at the top of the diagram. The cells are rotated by 45° and the  $\beta$ -FeSi<sub>2</sub> cell (dashed square) is placed on top of the Si cell where the top layer of atoms are indicated by the open circles.

The second possible  $\beta$ -FeSi<sub>2</sub>(100)/Si(001) interface (type B) lies at 45° to the orientation of type A. This is shown in Fig. 2. We redefine the  $\beta$ -FeSi<sub>2</sub> crystal translation vectors as  $b' = 2b$ ,  $c' = 2c$ , and  $a' = a$  and also for Si by the tetragonal cell  $a' = 3a$  and  $c' = c$ . We can see that the new surface unit cells in the interfacial planes [i.e.,  $\beta$ -FeSi<sub>2</sub>(100) and Si(001)] coincide with a maximum lattice mismatch of 4% where the  $\beta$ -FeSi<sub>2</sub> unit cell is expanded along the  $b$  and  $c$  directions. A smaller common surface unit cell can also be defined as shown by the dashed line in Fig. 2, which lies at 45° to the original cell. Since the  $b$  and  $c$  lattice parameters are not equal in  $\beta$ -FeSi<sub>2</sub> there is also a small angular mismatch of  $\pm 0.3\%$ . Since this cell and the one described above are equivalent, we use the smaller of these in the calculations.

We have performed calculations on a  $\beta$ -FeSi<sub>2</sub> cell, which is constrained to the Si lattice parameters (since it is the overlayer) defined by the interfaces described above. For the type-A interface, we constrained the  $b$  and  $c$  lattice parameters of  $\beta$ -FeSi<sub>2</sub> to the experimental value for the Si substrate, namely, 7.6792 Å [we shall refer to this as type A(I)]. However, for consistency, we also performed an identical calculation at the lattice parameter  $a = 5.39$  Å for Si, which was determined by our *ab initio* calculations using the same pseudopotential that was used in the  $\beta$ -FeSi<sub>2</sub> calculations

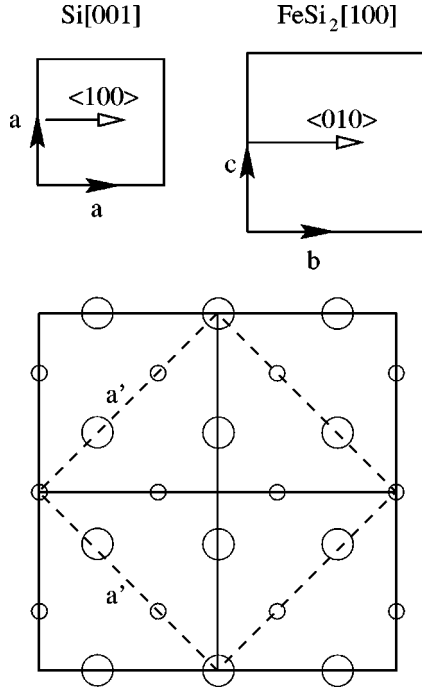


FIG. 2. Illustration of the type-B ( $\beta$ -FeSi<sub>2</sub>[010]||Si(001)) interface. The  $2 \times 2$  conventional  $\beta$ -FeSi<sub>2</sub>(100) surface cells are shown as full lines on top of the open circles indicating the top layer of atoms in the Si substrate. The lattice parameters  $b'$  and  $c'$  of the  $\beta$ -FeSi<sub>2</sub>(100) common unit mesh are given by  $b' = (0, 1, 1)b$  and  $c' = (0, -1, 1)c$ .

[this will be referred to as type A(II)]. For the type-B interface lattice constants,  $b$  and  $c$ , of the new constrained  $\beta$ -FeSi<sub>2</sub> overlayer cell were made equal to the side of the Si common unit mesh, 11.5188 Å.

In all cases the atomic positions were relaxed until the forces on the atoms were less than 0.001 eV/Å, which was

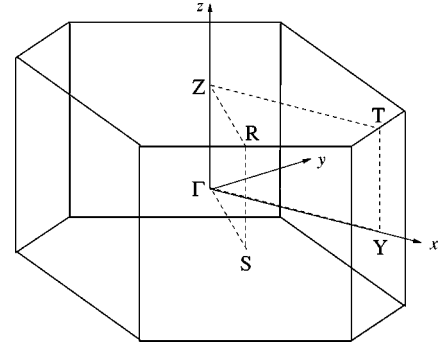


FIG. 3. Here we show the Brillouin zone of the the  $\beta$ -FeSi<sub>2</sub> structure (from the primitive unit cell) showing the lines along which the band structures shown in later figures were calculated.

consistent with our total-energy convergence criteria. The lattice parameters of the bulk  $\beta$ -FeSi<sub>2</sub> cell and the  $a$  lattice parameter of the constrained cells (which lies perpendicular to the interface) were also optimized in our calculations such that the uniaxial stress was less than 0.01 eV/Å<sup>3</sup>, which is consistent with the tolerance in the total energy of the system. The results of these calculations are summarized in Table I.

The structural parameters are in excellent agreement with available experimental results. It can be seen that the internal parameters remain fairly insensitive to changes in the lattice parameters as the fractional coordinate varies only in the third or fourth significant figure.

#### IV. ELECTRONIC STRUCTURE

For each structure of  $\beta$ -FeSi<sub>2</sub> considered here, we have calculated the electronic band structure along the lines indicated in Fig. 3. We show in Fig. 4 the calculated band structure of bulk  $\beta$ -FeSi<sub>2</sub> where all structural parameters have

TABLE I. The calculated and experimental (Ref. 3) structural parameters for  $\beta$ -FeSi<sub>2</sub> (space group Cmca) are given. The lattice parameters  $b$  and  $c$  (in Å) marked with \* are constrained to the underlying silicon lattice while  $a$  (in Å) is relaxed. The relaxed internal parameters are given in fractional coordinates of the unit cell.

| Structural parameters | Experimental | Bulk system | Type-A(I) | Type-A(II) | Type-B  |
|-----------------------|--------------|-------------|-----------|------------|---------|
| $a$                   | 9.863        | 9.8245      | 9.8643    | 9.9117     | 9.7933  |
| $b$                   | 7.791        | 7.7360      | 7.6792*   | 7.6084*    | 8.1450* |
| $c$                   | 7.833        | 7.9196      | 7.6792*   | 7.6084*    | 8.1450* |
| Fe(a)- $x$            | 0.2146       | 0.2181      | 0.2197    | 0.2141     | 0.2203  |
| Fe(a)- $y$            | 0.0          | 0.0         | 0.0       | 0.0        | 0.0     |
| Fe(a)- $z$            | 0.0          | 0.0         | 0.0       | 0.0        | 0.0     |
| Fe(b)- $x$            | 0.5          | 0.5         | 0.5       | 0.5        | 0.5     |
| Fe(b)- $y$            | 0.3086       | 0.3072      | 0.3101    | 0.3121     | 0.3062  |
| Fe(b)- $z$            | 0.1851       | 0.1846      | 0.1847    | 0.1819     | 0.3120  |
| Si(a)- $x$            | 0.1282       | 0.1285      | 0.1281    | 0.1285     | 0.1292  |
| Si(a)- $y$            | 0.2746       | 0.2742      | 0.2737    | 0.2762     | 0.2727  |
| Si(a)- $z$            | 0.0516       | 0.0523      | 0.0528    | 0.0529     | 0.0514  |
| Si(b)- $x$            | 0.3727       | 0.3730      | 0.3732    | 0.3735     | 0.3708  |
| Si(b)- $y$            | 0.0450       | 0.0456      | 0.0468    | 0.0480     | 0.0445  |
| Si(b)- $z$            | 0.2261       | 0.2270      | 0.2264    | 0.2242     | 0.2281  |

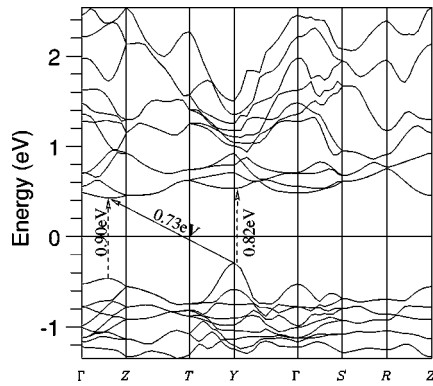


FIG. 4. The band structure of the fully relaxed bulk structure of  $\beta$ -FeSi<sub>2</sub> is shown along several lines of high symmetry. Arrows indicate the lowest-energy electronic band gaps. It can be seen (solid arrow) that the smallest band gap in this case is indirect between the Y point and the Z $\Gamma$  line.

been relaxed. It can be seen that the material is predicted to be semiconducting with an indirect band gap of 0.73 eV between the Y point in the valence band and 0.4 of the way along the Z $\Gamma$  line. This is in agreement with other *ab initio* calculations where an indirect gap was also reported, as discussed above.

However, most experimental measurements seem to indicate that the band gap should be direct. In practice,  $\beta$ -FeSi<sub>2</sub> is commonly made on a silicon substrate, therefore a direct comparison between the *ab initio* electronic structure calculated from the bulk structure where all structural parameters are allowed to relax and these experimental results is not strictly the correct comparison to make. Since the material is epitaxially grown on Si (usually for use in light emitting devices), the *b* and *c* lattice parameters are constrained. We have therefore also calculated the electronic structure  $\beta$ -FeSi<sub>2</sub> for a range of constrained structures.

For the type-B  $\beta$ -FeSi<sub>2</sub> where the *b* and *c* lattice parameters are expanded by approximately 4% with respect to the bulk case to fit the Si substrate, the band gap closes slightly as indicated in Fig. 5. The top valence band at the Y point rises in energy reducing the indirect gap to 0.53 eV and also reducing the direct gap at the Y point from 0.82 eV in the fully relaxed case to 0.62 eV. The quasidirect gap indicated by the dashed arrow in Fig. 5 along the Z $\Gamma$  line remains relatively unchanged at 0.83 eV.

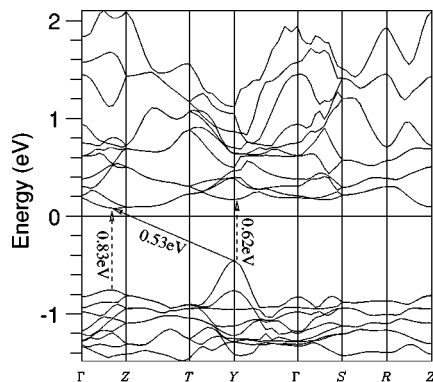


FIG. 5. The band structure of type-B  $\beta$ -FeSi<sub>2</sub> is shown here. The arrows indicate the smallest direct and indirect band gaps.

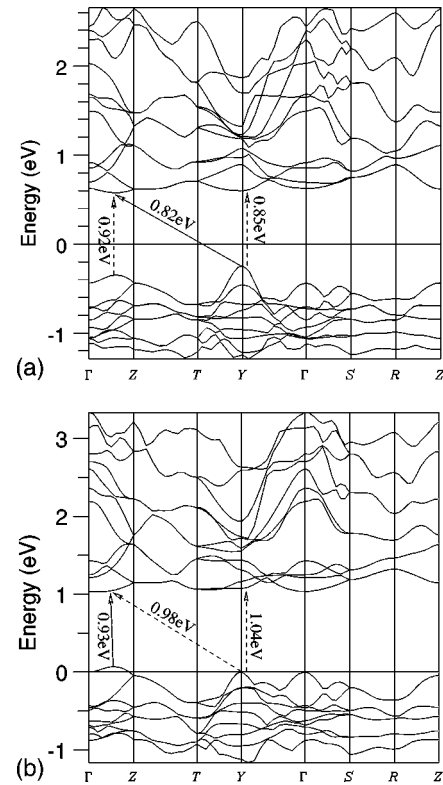


FIG. 6. (a) Band structure of type-A  $\beta$ -FeSi<sub>2</sub> constrained to the experimental lattice parameter of Si; (b) type-A  $\beta$ -FeSi<sub>2</sub> constrained to the *ab initio* lattice parameter of Si. The arrows indicate the smallest possible electronic band gaps, with the solid arrow showing the fundamental gap in each case. It can be seen that in the type-A(II) model the gap is direct whereas in type-A(I) and type-B (shown in Fig. 5), the gap is indirect, similar to the bulk unconstrained material.

For the type-A models, the *b* and *c*  $\beta$ -FeSi<sub>2</sub> lattice parameters are reduced by 1.4% and 1.8%, respectively to fit the Si substrate. The principle effect of this is to lower the energy of the top valence band at the Y point which signifi-

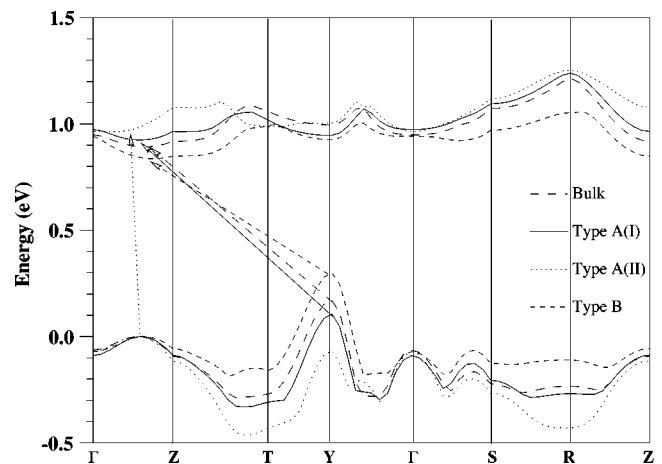


FIG. 7. The top valence band and bottom conduction band for each structure considered is shown here. We also plot the lowest energy gap for each case. It can be clearly seen that as the energy of the top band at the Y decreases, it favors the quasi-direct gap along the Z $\Gamma$  line.

cantly changes the electronic properties of the material. For the type-A(I) model, shown in Fig. 6(a), the direct and indirect gaps are 0.85 eV ( $Y$  point) and 0.82 eV ( $Y \rightarrow Z\Gamma$ ), respectively. More importantly, the difference in energy between the smallest direct and indirect band gaps is now only 30 meV compared to 90 meV for the bulk structure. The type-A(II) model, which corresponds to the purely *ab initio* simulation where the lattice parameter is constrained to the *ab initio* Si lattice parameter as opposed to the experimental value, the trend in the energy changes of the bands continues in the same direction [Fig. 6(b)]. The  $Y$  point energy reduces further going below the top of the valence band along the  $Z\Gamma$  line giving an almost direct gap of 0.93 eV. Similar to previous reports, we label this transition as *quasidirect* since it does not occur at a point of high symmetry. At the same time, the direct gap at  $Y$  has opened up to 1.04 eV and the indirect  $Y \rightarrow Z\Gamma$  gap becomes 0.98 eV.

To demonstrate the effect that the lattice parameter has on the band gap of the material, we show the top valence bands and bottom conduction bands together in the same diagram

(Fig. 7). The arrows in the figure indicate the lowest-energy transition, which is indirect from  $Y$  to  $Z\Gamma$  for the larger  $b$  and  $c$  cell parameters. As the unit cell is compressed the energy of the top valence band at  $Y$  rapidly decreases until it drops below the energy along the  $Z\Gamma$  line. At this point the transitions become quasi-direct.

In conclusion, we have calculated the electronic structure of  $\beta$ -FeSi<sub>2</sub> as a function of the lattice parameters as determined by the constraints of the substrate on which it is usually grown. We find that the electronic band gap depends sensitively on these parameters. The type-A material was found to favor a direct band gap while type-B and also the bulk material results in an indirect band gap 90 meV below the closest direct gap. Previous calculations on this material did not include the effect of strain on the lattice parameters which results in the range of behavior that have been reported. In some experimental studies of  $\beta$ -FeSi<sub>2</sub>, both direct and indirect gaps have also been reported but, again, this will depend critically on the methods used to prepare the material and the resultant state of strain.

- 
- <sup>1</sup>M.C. Bost and J.E. Mahan, J. Appl. Phys. **64**, 2034 (1998).  
<sup>2</sup>E. Arushanov, E. Bucher, Ch. Kloc, O. Kulikova, L. Kulyuk, and A. Siminel, Phys. Rev. B **52**, 20 (1995).  
<sup>3</sup>P.Y. Dusausoy, J. Protas, R. Wandji, and B. Roques, Acta Crystallogr., Sect. B: Struct. Crystallogr. Cryst. Chem. **B27**, 1209 (1971).  
<sup>4</sup>H.U. Nissen, E. Muller, H.R. Deller, and H. Vonkkanen, Phys. Status Solidi B **150**, 395 (1995).  
<sup>5</sup>J.L. Regolini, F. Trincat, I. Sagnes, Y. Shapira, G. Bremond, and D. Bensahel, IEEE Trans. Electron Devices **39**, 200 (1992).  
<sup>6</sup>C.A. Dimitriadis, J.H. Werner, S. Logothetidis, M. Stutzmann, J. Weber, and R. Nesper, J. Appl. Phys. **68**, 1726 (1990).  
<sup>7</sup>J.P. André, H. Alaoui, A. Deswarte, Y. Zheng, J.F. Pétrouff, X. Wallart, and J.P. Nys, J. Cryst. Growth **144**, 29 (1994).  
<sup>8</sup>N. Kobayashi, H. Katsumata, H.L. Shen, M. Hasegawa, Y. Makita, H. Shibata, S. Kimura, A. Obara, S. Uekusa, and T. Hatano, Thin Solid Films **270**, 406 (1995).  
<sup>9</sup>R. Eppenga, J. Appl. Phys. **68**, 3027 (1990).  
<sup>10</sup>N.E. Christensen, Phys. Rev. B **42**, 7148 (1990).  
<sup>11</sup>S. Eisebitt, J.-E. Rubensson, M. Nicodemus, T. Böske, S. Blügel, W. Eberhardt, K. Radermacher, S. Mantl, and G. Bihlmayer, Phys. Rev. B **50**, 18 330 (1994).  
<sup>12</sup>A.B. Filonov, D.B. Migas, V.L. Shaposhnikov, N.N. Dorozhkin, G.V. Petrov, V.E. Borisenko, W. Henrion, and H. Lange, J. Appl. Phys. **79**, 7708 (1996).  
<sup>13</sup>J. van Ek, P.E.A. Turchi, and P.A. Sterne, Phys. Rev. B **54**, 7897 (1996).  
<sup>14</sup>V. N. Antonov, O. Jepsen W. Henrion, M. Rebien, P. Stauss, and H. Lange, Phys. Rev. B **57**, 8934 (1998).  
<sup>15</sup>C. Giannini, S. Lagomarsino, F. Scarinic, and P. Castrucci, Phys. Rev. B **45**, 8822 (1992).  
<sup>16</sup>K. Radermacher, R. Carius, and S. Mantl, Nucl. Instrum. Methods Phys. Res. B **84**, 163 (1994).  
<sup>17</sup>T.D. Hunt, K.J. Reeson, K.P. Homewood, R.J. Wilson, R.M. Gwilliam, and B.J. Sealy, Nucl. Instrum. Methods Phys. Res. B **84**, 168 (1994).  
<sup>18</sup>D. Leong, M. Harry, K.J. Reeson, and K.P. Homewood, Nature (London) **387**, 686 (1997).  
<sup>19</sup>K.M. Geib, J.E. Mahan, R.G. Long, and G. Bai, J. Appl. Phys. **70**, 1730 (1991).  
<sup>20</sup>H.J. Monkhorst and J.D. Pack Phys. Rev. B **13**, 5188 (1976).  
<sup>21</sup>L. Kleinman and D.M. Bylander, Phys. Rev. Lett. **48**, 1425 (1982).  
<sup>22</sup>J.S. Lin, A. Qteish, M.C. Payne, and V. Heine, Phys. Rev. B **47**, 4174 (1993).  
<sup>23</sup>J.P. Perdew and Y. Wang, Phys. Rev. B **45**, 13 244 (1992).  
<sup>24</sup>D.M. Ceperley and B.J. Alder, Phys. Rev. Lett. **45**, 566 (1980); J.P. Perdew and A. Zunger, Phys. Rev. B **23**, 5048 (1981).  
<sup>25</sup>M.C. Payne, M.P. Teter, and J.D. Joannopolous, Rev. Mod. Phys. **64**, 1045 (1992).